Spin-Transport in Defective Graphene Nanoribbons

S.M.-M. Dubois,* G.-M. Rignanese, and J.-C. Charlier
Université catholique de Louvain,
Unité de Physico-Chimie et de Physique des Matériaux (PCPM),
European Theoretical Spectroscopy Facility (ETSF),
Place Croix du Sud 1, 1348 Louvain-la-Neuve, Belgium
(Dated: November 26, 2008)

Using first-principles calculations, the effect of magnetic point defects (vacancy and adatom) is investigated in zigzag graphene nanoribbons. The structural, electronic, and spin-transport properties are studied. While pristine ribbons display anti-parallel spin states at their edges, the defects are found to perturb this coupling. The introduction of a vacancy drastically reduces the energy difference between parallel and anti-parallel spin orientations, though the latter is still favored. Moreover, the local magnetic moment of the defect is screened by the edges so that the total magnetic moment is quite small. In contrast, when an adatom is introduced, the parallel spin orientation is preferred and the local magnetic moment of the defect adds up to the contributions of the edges. Furthermore, a spin-polarized transmission is observed at the Fermi energy, suggesting the use of such a defective graphene nanoribbon as spin-valve device.

PACS numbers: 61.46.-w, 71.15.Mb, 73.63.-b, 75.75.+a

Recent progresses in the preparation of contacted graphene mono-layer have enabled the synthesis of well-controlled nanometer-sized systems with open boundaries [1, 2]. Both one-dimensional graphene ribbons and zero-dimensional graphene dots have been achieved either by cutting exfoliated graphene layers [3, 4] or by patterning epitaxially grown graphenes [5]. Chemical methods have also been designed to achieve a solution-phase derivation of graphene ribbons with ultrasmooth edges [6]. These advances are at the origin of the raising interest in open boundary systems where the presence and shape of the edges influence drastically the π-electronic structure [7], opening the road towards new physical phenomena and technological applications.

As far as ribbons are concerned, the geometry of sp^2-bonded networks implies two possible cutting directions called "zigzag" and "armchair" according to the shape of the created edge. Due to topological reasons, zigzag-shaped edges give rise to peculiar extended electronic states which decay exponentially inside the graphene sheet [8, 9]. These edge-states, which are not reported along the armchair-shaped edges, come with a twofold degenerate flat band at the Fermi energy over one third of the Brillouin zone and have been suggested to be ferromagnetically ordered along the edge [10]. Recent DFT calculations on GNRs with zigzag-shaped edges (zGNRs), have suggested that due to the finite width of the ribbon, the interaction between the edges favors an opposite spin orientation at these edges [10, 11, 12]. These predictions are in agreement with the second Lieb's theorem [13] about the total spin in bipartite lattices.

Besides the possible magnetization of the edges, defect-induced magnetism is also expected in GNRs. Indeed, while many common topological defects (5/7 pairs, Stone-Wales [14],...) do preserve the saturation of the carbon atoms and are reported not to cause any local magnetization [15], processes where dangling bonds are created, may possibly induce a local magnetic moment [16, 17, 18]. For instance, carbon atoms can be removed from their lattice position, creating pairs of vacancies and adatoms. Such Frenkel defects are frequently present at thermal equilibrium [19, 20] in sp^2-bonded carbon systems. Depending on their positions, such magnetic point defects might affect differently the magnetic structure of GNRs. When located at the edge, these defects affect mainly the ferromagnetic order along the edge [21]. However, when located inside the ribbon, their effect on the magnetic structure is still an open issue.

In the present letter, magnetic point defects located in the vicinity of the ribbon axis have been used to tailor both the electronic and spin-transport properties of hydrogen passivated zGNRs. More specifically, the introduction of vacancy/adatom in these systems decreases the energy difference between the parallel and anti-parallel spin orientations of the edges. The magnetic moment of the vacancy defect is found to be drastically reduced in the defective ribbon compared to the ideal one. In the presence of carbon adatoms, a parallel spin orientation at the edges is favored, giving rise to a spin-polarized electronic transmission function around the Fermi energy.

Electronic irradiations can induce such magnetic point defects in graphene samples and allow to tune their number and their concentration [22]. Therefore, based on our theoretical predictions, one can hope to use defective zGNRs as spin-based nano-electronic devices.

Spin Polarized Density Functional Theory [23, 24] within the generalized-gradient approximation is used to investigate a hydrogen passivated 8-zGNR (width ~ 18Å). Periodic boundary conditions are used with fixed lateral dimensions which insure 25 Å of vacuum between the GNRs in neighboring cells. When vacancies or car-

bon adatoms are introduced, a 6×1×1 supercell is considered, leading to an nearest-neighboring defect distance of $\sim$ 15 Å and a defect concentration of $\sim$ 1%. Note that, for the computation of the transmission functions, a 22×1×1 supercell is considered in order to obtain a good screening of the perturbed Hartree potential due to the defect. In order to deal with the large number of atoms in the supercells, numerical atomic orbital basis set [25] are used to expand the wave-functions in conjunction with norm-conserving pseudo-potentials. The energy levels are populated using a Fermi-Dirac distribution with an electronic temperature of 250K. The integration over the 1D Brillouin zone is replaced by a summation over a regular grid of 40 k-points [26]. The geometry is fully relaxed until the forces on each atom, and on the unit cell [27] are less than 0.01 eV/Å and 0.05 eV/Å respectively. The small spin-orbit coupling of carbon atoms is neglected and independent collinear spin orientations, labeled α and β, are considered. Within such framework, the electronic ground state of the ideal 8-zGNR reveals anti-parallel ($\uparrow\downarrow$) spin orientations between the edges leading to a semiconducting band structure (0.5 eV band gap) with full spin degeneracy. On the other hand, the magnetic configuration with parallel ($\uparrow\uparrow$) spin orientations between the edges is found to be metastable (11 meV/edge-atom higher in energy). This configuration displays a metallic behavior, as the π^*_α and π_β bands are crossing at the Fermi energy, and presents a total magnetic moment of 0.51 μ_B per edge atom. These results are in good agreement with the previous calculations [10, 12].

By analogy with graphene, the removal of a carbon atom (vacancy creation) induces a Jahn-Teller distortion of the honeycomb structure. Two of the unsaturated carbon atoms come closer one to the other and form a weak covalent bond, inducing a pentagon like rearrangement. The third unsaturated carbon atom moves out of the plane [16, 28]. Consequently, the initial D_{3h} symmetry of the hexagonal network is lost in favor to the C_s symmetry [29]. In zGNRs, such atomic rearrangement leads to two possible orientations of the vacancy, called "perpendicular" and "tilted" according to the relative orientation of the mirror plane of the vacancy with respect to the ribbon axis.

As expected due to the presence of dangling bonds, the electronic density appears to be locally spin-polarized on the vacancy. The interaction between the magnetic moment of the defect and the spin ordered edge states results in four locally stable configurations for both vacancy orientations (see Fig. 1). In the following, the various magnetic configurations will be labeled X_Y, where X refers to the parallel ($\uparrow\uparrow$) or anti-parallel ($\uparrow\downarrow$) spin orientations between the ribbon edges, while Y refers to the parallel (P) or anti-parallel (AP) spin orientations between the defect and the nearest edge.

The energies related to the eight possible magnetic configurations of the vacancy are detailed in Table I. The tilted vacancy is found to be the most stable orientation, probably because of the formation of a stronger $C-C$ bond during the atomic reconstruction process. Consequently, the ribbon width displays a small shrinking (1.1%) around the vacancy, while a stretching is observed for the perpendicular vacancy orientation. Both vacancy orientations have the same $\uparrow\downarrow$ ground state as the pristine GNR. However, the energetics of the inter-edge coupling is modified, as shown in Table I. Indeed, while the energy difference between the parallel ($\uparrow\uparrow$) and anti-parallel ($\uparrow\downarrow$) spin orientations at the edges is 66 meV in the absence of defect, this value is reduced to 21 meV (44 meV) in the presence of a tilted (perpendicular) vacancy. At last, an accurate convergence study with respect to the size of the supercell allows us to predict a formation energy of 15.6 eV (which is approximately twice the one reported for the single vacancy in the graphene sheet [16, 18]) and a weak magnetic moment of 0.15 μ_B for the isolated vacancy in the tilted $\uparrow\downarrow_{AP}$ configuration.

At equilibrium, the carbon adatom is in a bridge-like position between two in-plane carbon atoms. This geometry is similar to the one reported for carbon atoms on graphene [16, 17, 29, 30, 31]. Again, in zGNRs, two adsorption sites are possible: labeled perpendicular or tilted

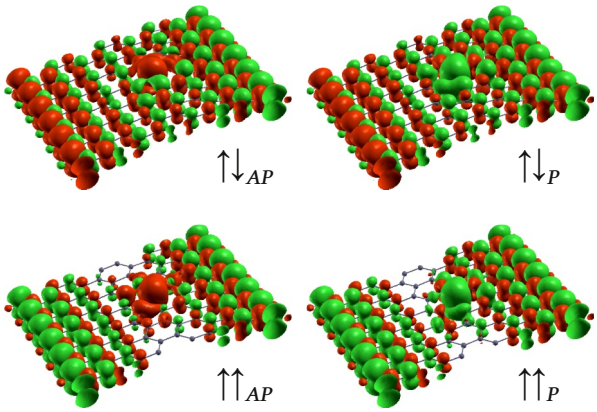

FIG. 1: [Color online] Spin polarized electronic densities ($\rho_\alpha - \rho_\beta$) isosurfaces for the four magnetic configurations associated to the tilted vacancy in zGNR. Green and yellow surfaces correspond to an excess of spin α and spin β electrons, respectively.

	Tilted vacancy		Perpendicular vacancy	
	ΔE (eV)	M_{tot} (μ_B)	ΔE (eV)	M_{tot} (μ_B)
$\uparrow\downarrow_{AP}$	0.000	0.19	0.110	1.98
$\uparrow\downarrow_{P}$	0.004	1.68	0.142	0.06
$\uparrow\uparrow_{AP}$	0.021	2.03	0.154	2.10
$\uparrow\uparrow_{P}$	0.023	4.06	0.170	4.52

TABLE I: Energies related to the ground state ($\uparrow\downarrow_{AP}$) and total magnetic moments associated to the eight possible magnetic configurations of the vacancy.

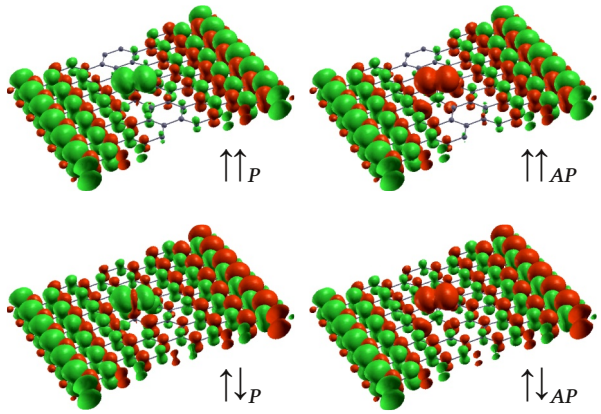

FIG. 2: [Color online] Spin polarized electronic densities ($\rho_\alpha - \rho_\beta$) isosurfaces for the four magnetic configurations associated to the carbon adatom in the tilted orientation. Green and yellow surfaces correspond to an excess of spin α and spin β electrons, respectively.

	Tilted adatom		Perpendicular adatom	
	ΔE (eV)	M_{tot} (μ_B)	ΔE (eV)	M_{tot} (μ_B)
$\uparrow\uparrow_P$	0.000	3.73	0.060	4.00
$\uparrow\uparrow_{AP}$	0.005	2.58	0.089	2.81
$\uparrow\downarrow_P$	0.008	0.11	0.094	0.72
$\uparrow\downarrow_{AP}$	0.032	0.67	0.094	0.72

TABLE II: Energies related to the ground state ($\uparrow\uparrow_P$) and total magnetic moments associated to the eight possible magnetic configurations of the carbon adatom.

depending on the orientation of the underlying carbon-carbon bond with respect to the ribbon axis. In both cases, the carbon adatom displays a local magnetic moment. In analogy with the vacancy case, the various magnetic configurations are labeled using the aforementioned X_Y syntax (see Fig. 2), and their corresponding energies are detailed in Table II.

The tilted $C-C$ bond is found to be the preferred host for carbon adsorption as it is associated with a smaller in-plane $C-C$ bond and a larger distance between the adatom and the ribbon. No significant shrinking is reported here. Similar to vacancies, carbon adatoms modify the energetics of the inter-edge coupling. However, this effect is enhanced in the presence of carbon adatoms and the $\uparrow\uparrow$ ground state is different from the one the pristine GNRs. Finally, an adsorption energy of 1.2 eV and a magnetic moment of 0.48 μ_B are computed for the isolated carbon adatom in the $\uparrow\uparrow_P$ configuration. These values are quite similar to the 1.40 eV and 0.45μ_B reported for the adsorption of carbon on graphene [16].

While the resulting ground states are different in the presence of a vacancy ($\uparrow\downarrow$) or a carbon adatom ($\uparrow\uparrow$), both defects induce the same trend on the inter-edge coupling. Indeed, the energy difference between the $\uparrow\downarrow$ and the $\uparrow\uparrow$ configurations in the presence of defects is found to be reduced well below the 66 meV predicted for the pristine ribbon. This result is a direct consequence of the defect-induced perturbation of the spin-polarized density. On one hand, by breaking the bipartite character of the carbon network, defects partially destroy the enhanced exchange splitting responsible of the stabilization of the $\uparrow\downarrow$ configuration [10]. On the other hand, as can be seen from Figs. 1 and 2 the spin polarization is larger in the center of the ribbon for the $\uparrow\downarrow$ configuration than for the $\uparrow\uparrow$ one. As a result, the density rearrangement is more limited around the defects in the former, which is confirmed by the projected density of states (not shown here). In summary, the introduction of defects induces a stabilization of the $\uparrow\uparrow$ configuration in contrast with the pristine case.

Since the introduction of magnetic point defects in zGNRs favors a specific spin configuration of the edges, a major impact is also expected on the transport properties of these 1D systems [32]. This will be investigated in the remainder of this letter. Our *ab initio* calculations of the electronic transmission functions, reported in Fig. 3, are performed within the Landauer approach. In order to simulate open boundary conditions, self-energies associated with the leads are included in the self-consistent calculation of the potential [33]. The supercell containing the point defect is connected to two leads consisting of a few unit cells of ideal zGNR [Fig. 3(a)]. Note that, as indicated above, a larger supercell has been used in order to ensure an accurate alignment of the electronic levels of the lead with those of the supercell.

As mentioned before, the $\uparrow\downarrow$ spin configuration of the pristine zGNR is preserved when an isolated vacancy is introduced. The defective zGNR remains semiconducting and its electronic transmission function displays a gap of 0.5 eV around the Fermi energy. On the contrary, in the presence of a carbon adatom, the $\uparrow\uparrow$ spin configuration is favored and the zGNR becomes metallic, inducing a non-zero electronic transmission function at the Fermi energy.

The main impact of the magnetic point defects on the transport properties is a global reduction of the transmission associated with the π and π^* electrons. This can be related to a decrease of the transmission probability of some π-π^* conduction eigenchannels compared to the pristine zGNR. For the vacancy [Fig. 3(b)], this effect appears essentially for energies ranging from -0.80 to -0.15 eV (π channels) and from 0.4 to 0.5 eV (π^* channels), inducing a slight breaking of the spin degeneracy. For the carbon adatom, a similar reduction of the transmission is found. But, defect-induced drops also appear at -0.3 eV and 0.02 eV. At these energies, states localized on the defect are present, which can only mix with the spin α conduction channel. Consequently, its transmission probability goes to zero due to the alteration of its π^* character and the spin-degeneracy of the electronic transmission function is lifted up just above the Fermi

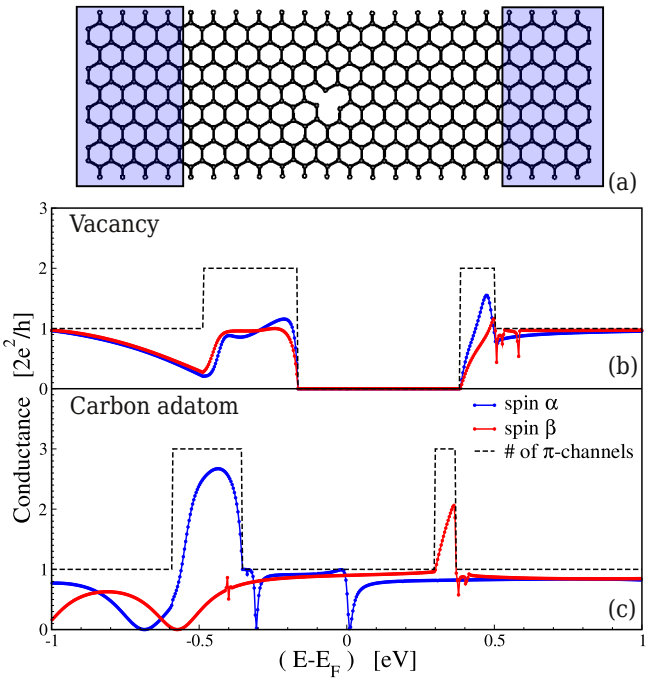

FIG. 3: [Color online] (a) Schematic representation of the model structure used to predict the electronic transmission functions of the zGNR in the presence of (b) an isolated vacancy in the $\uparrow\downarrow_{AP}$ configuration, and (c) an isolated carbon adatom in the $\uparrow\uparrow_{P}$ configuration. The spin α and spin β components are appear in blue and red, respectively, while the dotted line indicates the number of π channels.

energy.

In conclusion, the $\uparrow\uparrow$ spin configuration of zGNRs tends to be favored by the introduction of magnetic point-defects in the 1D system, as suggested by the low-energy spin-polarized density. The major impact of these point defects on the transport properties of zGNRs has been investigated. The predicted spin-polarized transmission function underlines the possibility to use adatom-doped graphene nanoribbons as valuable nano-devices in future spin-based electronics.

The authors acknowledge financial support from the F.R.I.A. (SMMD) and the F.R.S.-FNRS (JCC and GMR). Parts of this work are directly connected to the Belgian Program on Interuniversity Attraction Poles (PAI6) on "Quantum Effects in Clusters and Nanowires", to the ARC sponsored by the Communauté Française de Belgique and to the NANOQUANTA European Network of Excellence. Computational resources have been provided by the Université catholique de Louvain : all the numerical simulations have been performed on the LEMAITRE computer of the CISM.

* Electronic address: Simon.Dubois@uclouvain.be

[1] K. S. Novoselov *et al.*, Nature **438**, 197 (2005).
[2] C. Berger *et al.*, Science **312**, 1191 (2006).
[3] J. S. Bunch, Y. Yaish, M. Brink, K. Bolotin, and P. L. McEuen, Nano Lett. **5**, 287 (2005).
[4] A. K. Geim and K. S. Novoselov, Nat. Mater. **6**, 183 (2007).
[5] M. Y. Han, B. Özyilmaz, Y. Zhang, and P. Kim, Phys. Rev. Lett. **98**, 206805 (2007).
[6] X. Li, X. Wang, L. Zhang, S. Lee, and H. Dai, Science **319**, 1229 (2008).
[7] P. Koskinen, S. Malola, and H. Häkkinen, Phys. Rev. Lett. **101**, 115502 (2008).
[8] M. Fujita, K. Wakabayashi, K. Nakada, and K. Kusakabe, J. Phys. Soc. Jpn. **65**, 1920 (1996).
[9] K. Nakada, M. Fujita, G. Dresselhaus, and M. S. Dresselhaus, Phys. Rev. B **54**, 17954 (1996).
[10] H. Lee, Y.-W. Son, N. Park, S. Han and J. Yu, Phys. Rev. B **72**, 174431 (2005).
[11] H. Lee, N. Park, Y.-W. Son, S. Han and J. Yu, Chem. Phys. Lett. **398**, 207 (2004).
[12] Y.-W. Son, M. L. Cohen, and S. G. Louie, Phys. Rev. Lett. **97**, 216803 (2006).
[13] E. H. Lieb, Phys. Rev. Lett. **62**, 1201 (1989).
[14] A. J. Stone and D. J. Wales, Chem. Phys. Lett. **128**, 501 (1986).
[15] E. J. Duplock, M. Scheffler, and P. J. D. Lindan, Phys. Rev. Lett. **92**, 225502 (2004).
[16] P. O. Lehtinen *et al.*, Phys. Rev. Lett. **91**, 017202 (2003).
[17] P. O. Lehtinen, A. S. Foster, Y. Ma, A. V. Krasheninnikov, and R. M. Nieminen, Phys. Rev. Lett. **93**, 187202 (2004).
[18] O. V. Yazyev and L. Helm, Phys. Rev. B **75**, 125408 (2007).
[19] T.W. Ebbesen and T. Takada, Carbon **33**, 973 (1995).
[20] M. Kosaka, T.W. Ebbesen, H. Hiura, and K. Tanigaki, Chem. Phys. Lett. **233**, 47 (1995).
[21] M. Wimmer, I. Adagideli, S. Berber, D. Tománek, and K. Richter, Phys. Rev. Lett. **100**, 177207 (2008).
[22] P. Esquinazi *et al.*, Phys. Rev. Lett. **91**, 227201 (2003).
[23] J.M. Soler *et al.*, J. Phys.: Condens. Matter **14**, 2745 (2002).
[24] E. Artacho *et al.*, J. Phys.: Condens. Matter **20**, 064208 (2008).
[25] A numerical atomic orbital basis set of double-ζ plus one polarization and the 3s orbitals (DZP+3S) quality has been used for all the structural optimizations while the transmission functions have been obtained using basis set of single-ζ plus one polarization and the 3s orbitals (SZP+3S) quality.
[26] When the 6×1×1 and 22×1×1 supercells are used, the regular grid is reduced to 7 and 2 k-points, respectively, in order to achieve a similar degree of convergence.
[27] The force on the unit cell along the GNR axis is obtained by multiplying the corresponding stress by the surface of the unit cell in that direction.
[28] A. A. El-Barbary , R. H. Telling, C. P. Ewels, M. I. Heggie, and P. R. Briddon, Phys. Rev. B **68**, 144107 (2003).
[29] H. Amara, S. Latil, V. Meunier, P. Lambin, and J.-C. Charlier, Phys. Rev. B **76**, 115423 (2007).
[30] K. Nordlund, J. Keinonen, and T. Mattila, Phys. Rev. Lett. **77**, 699 (1996).
[31] Y. H. Lee, S. G. Kim, and D. Tománek, Phys. Rev. Lett. **78**, 2393 (1997).

[32] W. Y. Kim and K. S. Kim, Nature Nanotech. **3**, 408 (2008).
[33] A. R. Rocha *et al.*, Phys. Rev. B **73**, 085414 (2006).